Far-Field Optical Microscopy with a Nanometer-Scale Resolution Based on the In-Plane Image Magnification by Surface Plasmon Polaritons

Igor I. Smolyaninov,[1] Jill Elliott,[2] Anatoly V. Zayats,[2] and Christopher C. Davis[1]

[1]*Department of Electrical and Computer Engineering, University of Maryland, College Park, MD 20742, USA*

[2]*School of Mathematics and Physics, The Queen's University of Belfast, Belfast BT7 1NN, United Kingdom*

(Received 10 March 2004; published 7 February 2005)

A new far-field optical microscopy capable of reaching nanometer-scale resolution is developed using the in-plane image magnification by surface plasmon polaritons. This approach is based on the optical properties of a metal-dielectric interface that may provide extremely large values of the effective refractive index n_{eff} up to 10^3 as seen by surface polaritons, and thus the diffraction limited resolution can reach nanometer-scale values of $\lambda/2n_{\mathrm{eff}}$. The experimental realization of the microscope has demonstrated the optical resolution better than 60 nm at 515 nm illumination wavelength.

DOI: 10.1103/PhysRevLett.94.057401 PACS numbers: 78.67.−n, 07.60.Pb, 42.79.−e, 78.20.Ci

Optical microscopy is one of the oldest research tools. It dates back to 1609 when Galileo Galilei developed an *occhiolino* or compound microscope with a convex and a concave lens. Although various electron and scanning probe microscopes had long surpassed it in resolving power, optical microscopy remains invaluable in many fields of science. The reason for limited resolution of an optical microscope is diffraction of light waves and, ultimately, uncertainty principle: a wave cannot be localized much tighter than half of its wavelength $\lambda/2$. Immersion microscopes [1] have slightly improved resolution on the order of $\lambda_0/2n$ due to shorter wavelength of light λ_0/n in the medium with refractive index n. Nevertheless, immersion microscope resolution is limited by the narrow range of refractive indices n of available transparent materials which can be used as immersion media. For a while it was believed that the only way to achieve nanometer-scale spatial resolution optically is to avoid diffraction by detecting optical field in subwavelength proximity to a studied surface using a scanning near-field optical microscope [2]. Recently, some alternative approaches based on the idea of a "perfect lens" made from an artificial negative refractive index material have been proposed [3]. However, an image formed by a perfect lens would be observable only in the near-field of a perfect lens and would require an auxiliary near-field microscope. Although many fascinating results have been obtained in near-field optics, near-field microscopes are not as versatile and convenient to use as conventional far-field optical microscopes. For example, an image in a near-field optical microscopy is obtained by point-by-point raster scanning, which is a rather slow process.

In this Letter we present a new type of far-field optical microscopy, which is capable of reaching nanometer-scale resolution. We employ the two-stage microscope design in which a magnified planar image produced originally by surface plasmon polaritons (SPPs) in the metal surface plane is observed with a conventional optical microscope due to surface polariton coupling to light via random surface roughness or nanotailored surface defects. A planar metal-dielectric interface may provide at certain wavelengths extremely large values of the effective refractive index n_{eff}, as seen by propagating surface electromagnetic modes. Therefore, two-dimensional lenses or mirrors for SPPs exhibit strong focusing properties. The theoretical diffraction limit on resolution of such 2D optical element can be pushed down to nanometer-scale $\lambda_0/2n_{\mathrm{eff}}$ values. Used in reverse, such a microscope may become an optical lithography tool with nanometer-scale spatial resolution. We believe that the new technique will lead to numerous applications in biological imaging and subwavelength lithography.

Our approach is based on the fact that surface plasmon polaritons [4,5] may experience an extremely large effective refractive index on a metal-dielectric interface [6]. Let us assume that the metal film is bounded on both sides by the same dielectric and consider the dispersion law of SPPs. In such a case the dispersion law can be written as [7]

$$k^2 = \frac{\omega^2}{c^2}\frac{\epsilon_d \epsilon_m(\omega)}{\epsilon_d + \epsilon_m(\omega) \pm 2\epsilon_d e^{-kd}}, \qquad (1)$$

where $\epsilon_m(\omega)$ is the frequency-dependent dielectric constant of the metal. If we assume that (according to the Drude model) $\epsilon_m = 1 - \omega_p^2/\omega^2$, where ω_p is the plasma frequency of the lossless metal and d is large, the dispersion law can be simplified as

$$k^2 = \frac{\omega^2}{c^2}\frac{\epsilon_d \epsilon_m(\omega)}{\epsilon_d + \epsilon_m(\omega)}, \qquad (2)$$

where $\epsilon_m(\omega)$ is real. This dispersion law is shown in Fig. 1(b). The dispersion law (1) also looks very similar to Fig. 1(b) in the general case of a lossy metal film if the metal film thickness d is small, so that the imaginary part of the term $\pm 2\epsilon_d e^{-kd}$ compensates the imaginary part of ϵ_m. In such cases the plasmon wave vector k also diverges at some frequency, which is close to the frequency of

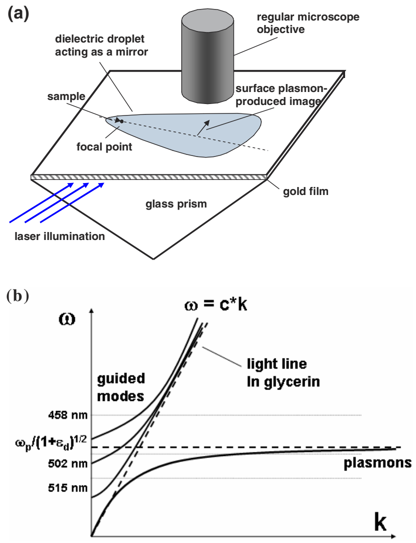

FIG. 1 (color online). (a) SPP-based far-field microscope: SPPs are excited by laser light and propagate inside a parabolically shaped droplet. Placing an object near the focus of a parabola produces a magnified image in the metal plane, which is viewed from the top with a conventional optical microscope. (b) SPP dispersion on the gold-glycerine interface and the positions of the Ar-ion laser lines. Also shown are the guided optical modes inside the thin layer of glycerine.

surface plasmon resonance $\omega_0 = \omega_p/(1+\epsilon_d)^{1/2}$. In other words, near this frequency the effective refractive index n_{eff} for surface plasmon polaritons becomes extremely large. Because of this divergence, near the frequency of SP resonance, a droplet of a liquid dielectric on a metal surface behaves as a very strong lens for surface polaritons propagating through the droplet. On the other hand, the droplet boundary becomes an efficient mirror for surface polaritons propagating inside the droplet at almost any angle of incidence due to the total internal reflection (this leads to the ''black hole'' analogy described in [6]). Since the SPP wavelength λ_{sp} observed in the experiments may be as small as a few nanometers [8,9] (hence n_{eff} may reach extremely large values up to 10^3), the theoretical diffraction limit of resolution of such lenses and mirrors is about $\lambda_{sp}/2$ and theoretically may reach a scale of a few nanometers. Although the Ohmic losses in a metal limit the range of observable short-wavelength SPPs and their propagation length, in the symmetric geometry, the film thickness can be chosen to achieve desirable wavelength and increase propagation length at a given frequency using the SPPs with antisymmetric electric field configuration [4,10].

Let us consider a two-dimensional SPP microscope made of appropriately shaped planar dielectric droplet [Fig. 1(a)]. The short-wavelength SPPs can be launched inside the droplet by the illuminating light due to diffraction on a surface object located inside the droplet [Fig. 1(a)]. The diffraction will provide the wave vector conservation for light coupling to SPPs. (Alternatively, the object can be illuminated by the SPP beam excited inside the droplet by another object.) A 2D magnified image of the object will be formed by SPPs in the appropriate location on the metal surface. Because of the metal surface roughness and the Raleigh scattering in the dielectric, SPPs are partially scattered into photons above the prism and can be observed with a conventional optical microscope. The image brightness far exceeds the background of scattered SPPs in other areas of the surface due to higher energy concentration. In addition, a fluorescence scheme of the SPP field visualization using far-field optical microscopy may be used [11]. As a result, the two-stage microscope arrangement is realized: SPPs produce an enlarged 2D image on the metal surface which then is observed with a conventional optical microscope. Thus, the goal of a 2D SPP microscope design is to provide sufficiently high 2D image magnification, so that all the 2D image details would be larger than the $\lambda_0/2$ resolution limit of the conventional optical microscope. In this way, far-field optical microscopy with nanometer-scale resolution can be achieved.

In the experimental scheme similar to one described in Ref. [6], glycerin microdroplets have been used as 2D optical elements for SPPs. The dielectric constant of glycerin $\varepsilon_g = 2.16$ is ideally suited for experiments performed on a gold surface [12] within the wavelength range of the emission lines of an argon-ion laser [Fig. 1(b)]. According to Eqs. (1) and (2), at the light wavelength $\lambda_0 = 502$ nm, the corresponding SPP wavelength on the gold-glycerin interface is $\lambda_{sp} \approx 70$ nm, and $n_{\text{eff}} = \lambda_0/\lambda_{sp} \approx 7$. Since glycerin dielectric constant is very close to the dielectric constant of the SiO_2 substrate, the symmetric environment is realized, and the SPP propagation length is estimated as ~ 10 μm for the film thickness 40 nm and ~ 40 μm for the film thickness 20 nm. It should be noted that the interaction with guiding modes [Fig. 1(b)] in the dielectric may further increase the propagation length [10]. Thus, subwavelength spatial resolution of the optical microscope around 500 nm wavelength may be realized. However, the achievable resolution is strongly frequency-dependent due to the dispersion of the dielectric constant of metal (e.g., SPPs cannot be excited at the 458 nm wavelength of an argon-ion laser).

In our experiments the studied objects were immersed inside glycerin droplets on the thin gold film surface. The droplets were formed in desired locations by bringing a probe wetted in glycerin into close proximity to a sample. The size and location of the droplets were controlled by the probe movement observed with a conventional microscope. This technique allows formation of droplet with shapes reasonably close to parabolic, and the droplet boundary serves as a 2D parabolic mirror for propagating SPPs excited inside the droplet. Since the SPP wavelength is much smaller than the droplet sizes, the image formation in such a mirror can be analyzed by simple geometrical optics. In the first experiment, a set of seven artificial pinholes in a gold film was produced inside a glycerin droplet using a sharp STM tip. Such pinholes are known to ''emit'' directional SPP beams under external illumination [13]. Observed in a conventional optical microscope, such structure is brighter in the areas where SPP are scattered in light. This arrangement of the pinholes and the droplet produces demagnified images (*a, b*) of the two brightest pinholes near the ends of the scratch (*A, B*). The scattered light is stronger in the image locations due to stronger SPP field at these locations. The position of the focus of the parabolic droplet edge was found from the known edge geometry and geometrical optics considerations as shown by a green dot in Fig. 2(b). Given the focus location, ray optics was used to show that the brightest pinholes *A* and *B* are imaged into the points *a* and *b*. Such demagnified (down to $\lambda_{sp}/2$) images produced by SPP may be used in subwavelength optical lithography.

To check the imaging properties of the microscope, various arrangements of nanoholes in a metal film were studied. Illuminated by laser light at appropriate wavelength, nanohole arrays excite the SPP modes on a structured surface [4,5]. Figure 3 shows various degrees of 2D image magnification obtained with a $30 \times 30\ \mu\mathrm{m}^2$ rectangular nanohole array with 500 nm hole spacing described in Ref. [14]. In general, smaller glycerine droplets produced higher magnification in the images. It should be pointed out that all the guided modes in the droplet [Fig. 1(b)] participate in the formation of the 2D images. The relative contribution to the image of each mode changes with distance from the imaged object due to varying mode coupling and decay. The image reconstructions via 2D ray tracing are in good agreement with the experimental images. Figures 3(c)–3(f) obtained using $\lambda_0 = 502$ nm demonstrate that the rows of nanoholes separated by 500 nm are resolved in the image Fig. 3(c) obtained using only a 10× magnification of the conventional microscope; at the same time, individual 150 nm diameter nanoholes are resolved in the image Fig. 3(e). These nanoholes are located in close proximity to the focus of the droplet-mirror, and hence have the highest image magnification. The cross section Fig. 3(g) through the row of nanoholes in Fig. 3(e) indicates edge resolution of at least 100 nm. Images taken in the same geometry with light of 458 nm wavelength, at which no SPPs can be excited, show drastic reduction in resolution [cf. Figs. 3(g) and 3(h)]. The same as in conventional optics, the position of the object with respect to the focus of the mirror determines the resemblance between the image and the object. The strong image distortions are observed since the size of the object is comparable with the mirror size, and different parts of the object are in significantly different locations with respect to the focus. Imperfections of the droplet edge, same as imperfections of conventional lenses and mirrors, lead to the reduction in image brightness and aberrations. However, the use of liquid droplets makes sure that the edge imperfections on the most important scale compatible with the SPP wavelength (which may cause strong SPP

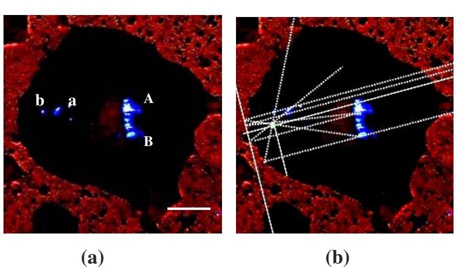

FIG. 2 (color online). (a) Image demagnification by a SPP mirror. (b) Ray optics is used to show that the pinholes *A* and *B* in (a) artificially created inside a glycerine droplet are imaged into *a* and *b*, which are located near the geometrically defined position of the focus [shown by the green dot in (b)]. The scale bar is 7 μm.

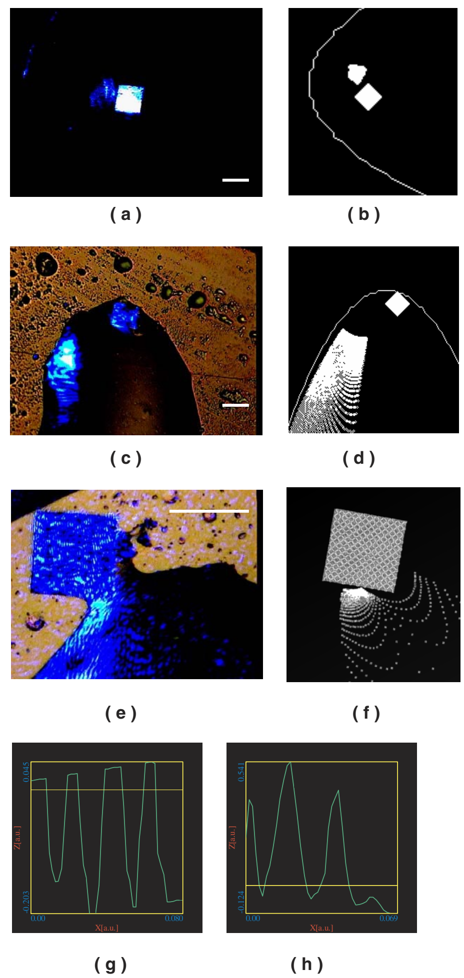

FIG. 3 (color online). (a), (c), (e) 2D images of a $30 \times 30\ \mu\mathrm{m}^2$ rectangular nanohole array with 500 nm hole spacing, obtained with SPPs excited with $\lambda_0 = 502$ nm using various glycerine droplets as SPP optical elements. The scale bars are 30 μm. (b), (d), (f) Image reconstructions via ray tracing of SPP in droplets. Individual nanoholes of the array are shown as individual dotes in model images. The cross section (g) through the row of nanoholes in (e) shows the edge resolution of at least 100 nm. (h) The spatial resolution is lost with $\lambda_0 = 458$ nm at which SPPs are not excited.

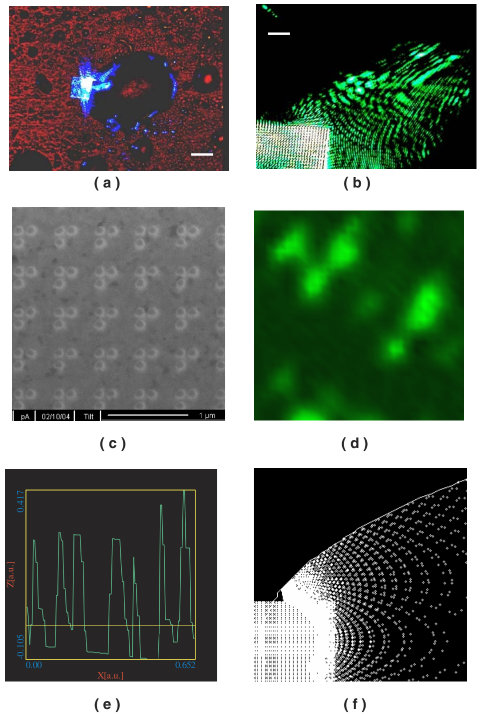

FIG. 4 (color online). Resolution test of the microscope. The $30 \times 30\ \mu m^2$ array of triplet nanoholes (100 nm hole diameter, 40 nm distance between the hole edges in the triplet, 500 nm period) shown in (c) is imaged using a SPP optical element formed by a glycerine droplet (a). (b) The image of the triplet array obtained at $\lambda_0 = 515$ nm and (f) its ray-tracing reconstruction. The scale bar is 30 μm in (a) and 5 μm in (b). (d) Magnified image shows subwavelength triplet structure. (e) The cross section through the line of nearest nanoholes.

scattering) are virtually absent due to surface tension. The strongest aberration effects may be caused by the multiple SPP reflections produced by the droplet boundary. However, due to small SPP propagation length only the portion of the boundary nearest to the sample participates considerably in the image formation. While the actual shape of the glycerin droplet was difficult to control in the first experiments, more advanced fabrication, such as preliminary microstructuring of the surface in parabolic or elliptical shapes, may be used in the future to control droplet shapes.

It should be noted that as far as imaging of periodic samples is concerned, diffraction gratings are known to reproduce their illumination patterns at some set of periodic distances from the grating (the Talbot effect). However, in the case under consideration it seems highly improbable that the periodicity of the source would exactly coincide with the periodicity of the Talbot planes spacing in order to explain the resolution observed.

A resolution test of our microscope has been performed using a $30 \times 30\ \mu m^2$ array of triplet nanoholes [Fig. 4(c): 100 nm hole diameter with 40 nm distance between the hole edges in the triplet, and 500 nm spacing between triplets]. The image of the triplet array measured with $\lambda_0 =$ 515 nm wavelength [Fig. 4(b)] was obtained using an SPP optical element formed by a glycerine droplet shown in Fig. 4(a). Although the expected resolution of the microscope at 515 nm is somewhat lower than at 502 nm, the 515 nm laser line is brighter and the excited SPPs experience lower Ohmic losses, which allowed us to obtain higher contrast in the 2D image. The triplet nanohole structure of the sample is clearly visible [Fig. 4(d)]. The cross-sectional analysis through the nearest holes [Fig. 4(e)] clearly indicates spatial resolution of at least 60 nm (better than $\lambda_0/8$). Theoretical resolution of the described microscopy approach may reach a few nanometer scale if dielectric material and wavelength are appropriately chosen. Such a microscope has a potential to become an invaluable tool in medical and biological imaging, where far-field optical imaging of individual viruses and DNA molecules may become a reality (the hole arrays can be used as "light" sources to produce short-wavelength SPPs for imaging of objects on a surface). It allows very simple, fast, robust, and straightforward image acquisition. Moreover, water droplets on a metal surface can be used as elements of SPP optics in measurements where an aqueous environment is essential for biological studies. In addition, used in reverse, such a microscope may be used in nanometer-scale optical lithography.

This work has been supported in part by the NSF Grants No. ECS-0210438 and No. ECS-0304046 and EPSRC (UK).

[1] R. R. Kingslake, *Optical System Design* (Academic Press, London, 1983).
[2] *Near Field Optics*, edited by D. W. Pohl and D. Courjon (Kluwer, Dordrecht, 1993).
[3] J. B. Pendry, Phys. Rev. Lett. **85**, 3966 (2000).
[4] H. Raether, *Surface Plasmons* (Springer, Berlin, 1988).
[5] A. V. Zayats and I. I. Smolyaninov, J. Opt. A Pure Appl. Opt. **5**, S16 (2003).
[6] I. I. Smolyaninov, New J. Phys. **5**, 147 (2003); I. I. Smolyaninov and C. C. Davis, Phys. Rev. B **69**, 205417 (2004).
[7] J. J. Burke, G. I. Stegeman, and T. Tamir, Phys. Rev. B **33**, 5186 (1986).
[8] I. I. Smolyaninov, V. S. Edelman, and V. V. Zavyalov, Phys. Lett. A **158**, 337 (1991).
[9] H.-J. Maas, J. Heimel, H. Fuchs, U. C. Fischer, J. C. Weber, and A. Dereux, J. Microsc. **209**, 241 (2002).
[10] A. V. Zayats, J. Eliiott, I. I. Smolyaninov, and C. C. Davis (to be published); I. I. Smolyaninov, cond-mat/0405098.
[11] H. Ditlbacher, J. R. Krenn, G. Schider, A. Leitner, and F. R. Aussenegg, Appl. Phys. Lett. **81**, 1762 (2002).
[12] The dielectric constant of gold can be found in *CRC Handbook of Chemistry and Physics*, edited by R. C. Weast (CRC Press, Boca Raton, 1987).
[13] I. I. Smolyaninov, D. L. Mazzoni, and C. C. Davis, Phys. Rev. Lett., **77**, 3877 (1996).
[14] A. V. Zayats, I. I. Smolyaninov, W. Dickson, and C. C. Davis, Appl. Phys. Lett. **82**, 4438 (2003).